Audio Engineering Society

Convention Paper 9712

Presented at the 142nd Convention
2017 May 20–23, Berlin, Germany

This convention paper was selected based on a submitted abstract and 750-word precis that have been peer reviewed by at least two qualified anonymous reviewers. The complete manuscript was not peer reviewed. This convention paper has been reproduced from the author's advance manuscript without editing, corrections, or consideration by the Review Board. The AES takes no responsibility for the contents. This paper is available in the AES E-Library (http://www.aes.org/e-lib), all rights reserved. Reproduction of this paper, or any portion thereof, is not permitted without direct permission from the Journal of the Audio Engineering Society.

The influence of symmetrical human ears on the front-back confusion

Ramona Bomhardt[1] and Janina Fels[1]

[1]*RWTH Aachen University, Institute of Technical Acoustics, Medical Acoustics Group, 52074 Aachen, Germany*

Correspondence should be addressed to Ramona Bomhardt (rbo@akustik.rwth-aachen.de)

ABSTRACT

Human beings have two ears to localize sound sources. At a first glance, the dimensions of the right and left ears are generally very similar. Nevertheless, the individual anthropometric dimensions and shape of both ears are disparate. These differences improve localization on the cone of confusion where interaural differences do not exist. To determine the influence of asymmetric ears, individual HRTF data sets are analytically and subjectively compared with their mirrored versions.

1 Introduction

Binaural reproduction techniques using head-related transfer functions (HRTFs) require spatial high-resolution data sets of individually measured HRTFs for an optimal localization performance. However, the technical effort to measure these HRTF data sets is tremendous. In contrast to this, non-individual HRTF data sets deteriorate the localization performance [1]. Since the HRTF is mainly influenced by the torso, head and ear geometry, the individual HRTFs can be estimated using individual anthropometric dimensions to reduce the measurement effort and enhance the localization performance compared to non-individual HRTFs [2, 3, 4, 5, 6]. To further simplify the measurement effort, the question arises, whether it is sufficient to assume symmetric ears. As shown in Fig. 1, both ears are often very similar but differ in detail.

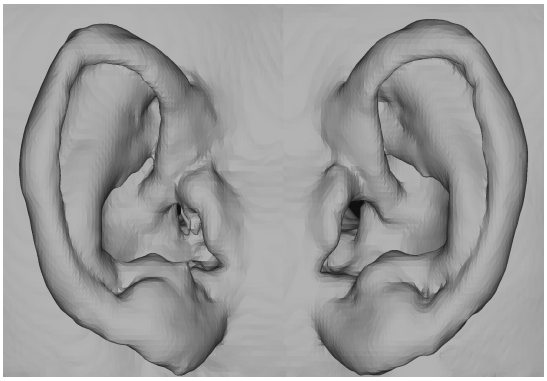


Fig. 1: The three-dimensional ear models (right and left) of subject #33 from the ITA HRTF database [7].

The complex ear geometry provides important monaural cues to localize sources on the cones of confusion. On these cones, binaural cues such as the interaural

time and level difference are absent, whereby interference effects of the torso, head and pinna are used to specify the source position. However, the auditory system is not always able to interpret these high frequency cues at which front-back confusions occur [8, 9, 10, 1]. Especially a static head position, the absence of high frequencies and binaural reproduction techniques with non-individual HRTFs make these confusions more probable.
To study the asymmetry of the human ears, the ears and corresponding head-related transfer functions (HRTFs) from the HRTF database of the Institute for Technical Acoustics (RWTH Aachen University) are used in this study [7]. This database provides detailed three-dimensional ear models with corresponding high-resolution HRTF data sets. Afterwards, the influence of the symmetry on the front-back confusion rate is examined.

2 Symmetry of the anthropometric dimensions

Given that the anthropometric dimensions and the monaural cues are linked, the symmetry of the anthropometric dimensions is investigated in this section. The shape of the cavum concha, for instance, influences the first and second resonance of the pinna [11, 12]. The standing wave shapes at higher frequencies are complex and also involve the fossa. On the other hand, direction-dependent destructive interference effects are introduced by rim structures such as the helix or antihelix [13].
Since three-dimensional ear models of the right and left ears cannot be compared directly, one-dimensional anthropometric dimensions are extracted (see Tab. 1 and Fig. 2) according to the CIPIC specifications [14]. The manually-detected measurement points cause measurement uncertainties of about 1 mm (repeated measurements) due to the complex shape of the ear. Additionally, the definition of the measurement points, as shown in Fig. 2, deviates due to the individual characteristic shape of the ear.

	d_1	d_2	d_3	d_4	d_5	d_6	d_7
Mean	17	9	18	19	64	36	6
Std.	2	2	3	3	5	3	1
Min	13	5	13	13	53	30	4
Max	22	11	28	25	74	43	10
Dev.	24	44	33	32	16	17	33

Table 1: The subject-dependent statistical evaluation of the ear dimensions in millimeters according to the CIPIC specifications and their percentage deviations (2 Std./Mean).

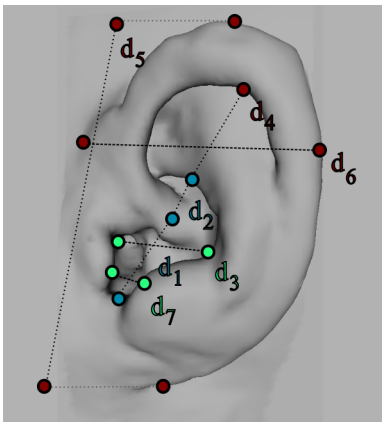


Fig. 2: The anthropometric dimensions are extracted from the three-dimensional ear models according to the CIPIC specifications, as shown for the left ear of subject #17.

The measured dimensions are statistically summarized for all subjects and ears in the present database in table 1. The ear height d_5 and width d_6 are the largest dimensions, followed by the fossa height d_4 as well as the cavum concha height d_1 and width d_3. The largest inter-subject deviations are found for the cymba concha height d_2.
To evaluate the difference between the right and left ear dimensions, the subject-dependent anthropometric dimensions of both ears are subtracted $|d_L - d_R|$ as in table2. This highlights the fact that the large dimensions such as d_4, d_5 and d_6 also show the considerable deviations between both ears. The smaller the dimension, the greater the relative difference and the lower the correlation coefficient ρ_{LR}. However, it cannot be clarified whether these higher correlations are caused by measurement uncertainties or deviating ear geometry.

3 Symmetry of the head-related transfer functions

The major impact on the front-back confusion rate can be ascribed to monaural cues above 7 kHz [1]. Therefore, the asymmetry of the low frequency ITD is neglected [15], and spectral difference as well as high

	d_1	d_2	d_3	d_4	d_5	d_6	d_7
Δ_{abs}	1	1	1	2	2	2	1
Δ_{max}	4	4	6	6	5	5	4
Δ_{rel}	7	14	8	9	3	4	23
ρ_{LR}	0.6	0.6	0.8	0.8	0.9	0.8	0.3

Table 2: Comparison of the dimensions of the right and left ear. The averaged absolute difference $\Delta_{abs} = |d_L - d_R|$ and maximum difference $\Delta_{max} = \max|d_L - d_R|$ are given in millimeters. The relative difference $\Delta_{rel} = |d_L - d_R|/d_L \cdot 100$ is expressed in percentage.

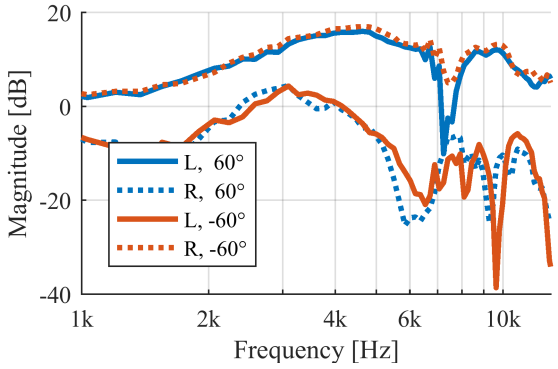


Fig. 3: Measured HRTFs at symmetric positons $(\theta, \varphi) = (0°, \pm 60°)$ for the left (L) and right (R) ear of subject #33.

frequency interference effects are examined in the following. These include resonances as well as destructive interferences which can be detected as local maxima or minima of the HRTF.

Each HRTF of a data set in the database is related to a specific sound direction (θ, φ). Thereby, $-90° \leq \theta \leq 90°$ specifies the elevation angle and $-180° \leq \varphi \leq 180°$ specifies the azimuth angle in a mathematical coordinate system. The x-axis of this coordinate system is defined by a vector from the right to the left ear canal entrance. The y-axis points towards the nose and defines the direction $(0°, 0°)$. Assuming a symmetric head around the yz-plane, the so-called median plane, the HRTFs of the directions $\varphi = 60°$ of the left ear are symmetric to the ones of the directions $\varphi = -60°$ of the right ear. While at lower frequencies both HRTFs are almost similar, they deviate at higher frequencies based on asymmetries of the head and ear. These differences are shown in Fig. 3 where the right and left ear HRTFs of these directions are plotted. However, deviations can also be introduced during the measurement by a non-ideally aligned subject.

3.1 Inter-ear spectral difference

To investigate the asymmetry of a whole HRTF data set, the inter-subject spectral difference ($\overline{\text{ISSD}}$) by Middlebrooks [3], which determines the difference between two HRTF data sets, is used to express the inter-ear spectral difference ($\overline{\text{IESD}}$). For this the HRTF data set is split into HRTFs of the left ear HRTF_L and right ear HRTF_R. To compare symmetric directions $\pm\varphi$, the azimuth angles of the HRTF_R have to be mirrored $\varphi_M = 360° - \varphi_R$. Subsequently, the difference between these two subsets is characterized by the variance of the frequency-dependent ratio $|\text{HRTF}_{L,i}(f_j)|/|\text{HRTF}_{R,i}(f_j)|$. The variance over the frequencies is averaged over all directions n_{dir}

$$\overline{\text{IESD}} = \frac{1}{n_{dir}} \sum_{i=1}^{n_{dir}} \text{var}\left(20\log_{10}\frac{|\text{HRTF}_{L,i}(f_j)|}{|\text{HRTF}_{R,i}(f_j)|}\right). \quad (1)$$

In contrast to the $\overline{\text{ISSD}}$ by Middlebrooks [3], which is calculated for 64 frequency bands in the range of 3.7 to 12.9 kHz, the presented $\overline{\text{IESD}}$ is calculated for each frequency bin f_j between 4 to 13 kHz. Additionally, the Middlebrook's study used DTFs instead of HRTFs, which does not influence the IESD much, since the variance is determined. The resulting averaged variation between right and left ear amounts to $22 \pm 8\,\text{dB}^2$ between 3 kHz and 13 kHz. As a comparison, the overall $\overline{\text{ISSD}}$ of all subjects of the database is $37 \pm 10\,\text{dB}^2$.

To investigate the deviations between the right and left HRTFs per frequency, the second frequency measure $\text{IESD}(f)$ is used in the following. Similar to the $\overline{\text{ISSD}}$, the ratio between the right and left ear HRTFs is calculated first, and subsequently the standard deviation of all directions is determined in such a way that the $\text{IESD}(f)$ is frequency-dependent

$$\text{IESD}(f_j) = \sigma\left(20\log_{10}\frac{|\text{HRTF}_{L,i}(f_j)|}{|\text{HRTF}_{R,i}(f_j)|}\right). \quad (2)$$

The resulting averaged $\text{IESD}(f)$ over all subjects of the database is shown in Fig. 4 and features an increasing mismatch towards higher frequencies. While the $\text{IESD}(f)$ at lower frequencies below 5 kHz is about 2 dB, it increases especially in the range between 6 and 9 kHz. This increasing difference can be ascribed to destructive interferences which are observable as notches

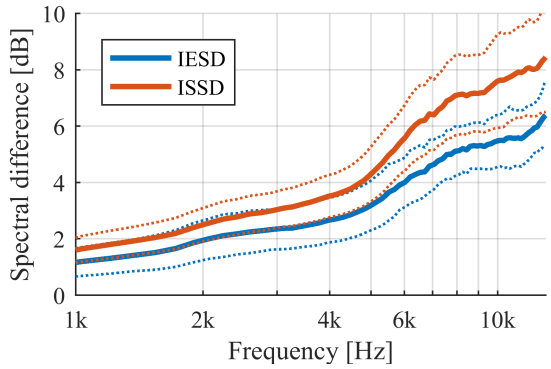


Fig. 4: The solid line of the frequency-dependent inter-ear and inter-subject difference mark the mean of all subjects. The dotted lines show the corresponding standard deviations.

of the HRTFs. In comparison, the frequency-dependent IESD is lower than the ISSD, as already observed for the direction-averaged $\overline{\text{IESD}}$ and $\overline{\text{ISSD}}$. However, the IESD is similar to the spectral difference between two repeated measurements of one subject.

3.2 Detection of the first resonance

The first resonance of the ear provides an almost direction-independent maximum that can be determined by a local maximum search. This maximum is sometimes influenced by a notch or measurement noise, for which reason spatial averaging provides a more robust detection of the first peak (cf. Mokhtari and colleagues [16]). The resulting subject-averaged resonance frequency of the database is 4.3 ± 0.7 kHz and varies due to the different cavum concha shapes. Comparing the resonances of the right and left data sets shows on average no difference. This implies that there is no general deviation of one ear side. However, the standard deviation between both sides amounts to 0.3 kHz with strong correlation $\rho_{LR} = 0.9$ between both. Considering the studies of Roffler and Butler [9] or Bronkhorst [1], the confusion rate is clearly reduced by providing frequency cues above 7 kHz. For this reason it is assumed that the first resonance frequency has a low impact on the confusion rate.

3.3 Detection of destructive interference

Destructive interferences are relevant on the cones of confusion and appear as frequency- and direction-dependent notches in the HRTFs. While Raykar and colleagues [17] detected these notches analyzing the group delay in the time domain, Spagnol and colleagues [18] used a tracking and minimum detection strategy. In the present section a tracking strategy is presented which detects the notches with the aid of a local minimum search in combination with a Kalman filter:

	Mean $\pm$ std.	Δ_{LR} (mean $\pm$ std.)	ρ_{LR}
f_R	4.3 ± 0.7 kHz	0 ± 0.3 kHz	0.9
$f_{N,10°}$	7.2 ± 0.6 kHz	0 ± 0.5 kHz	0.6
$f_{N,30°}$	7.4 ± 0.6 kHz	0 ± 0.6 kHz	0.5
$f_{N,60°}$	8.0 ± 0.8 kHz	-0.1 ± 0.6 kHz	0.7
$f_{N,70°}$	8.3 ± 0.8 kHz	0 ± 0.5 kHz	0.8

Table 3: The resonance frequencies f_R as well as the notch frequencies f_N at different azimuth angles θ in the horizontal plane are shown. In addition, the difference Δ_{LR} between the right and left ear as well as their correlation ρ_{LR} are listed.

1. The ipsilateral HRTFs are extracted from an HRTF data set for a single azimuth angle φ, since the notch is less pronounced for contralateral HRTFs.

2. A local minimum detection is applied on these elevation-dependent transfer functions between 3 kHz and 11 kHz under the assumption that the minimum has to be smaller than 5 dB and is well pronounced (cf. Fig. 5 and 6).

3. A Kalman filter is exploited as a tracking algorithm for the first notch. This has the advantage that uncertainties, which occur due to measurement noise or resonances, can be suppressed. In general, the notch frequency increases with an increasing elevation angle. It can be observed between $\theta = -60° \ldots 30°$ and frequencies between $f = 5 \ldots 9$ kHz for most of the ipsilateral HRTFs. Therefore, an initial position around $\theta_0 = -60°$ and $f_0 = 6$ kHz is used to detect the first notch using the Kalman filter. The following positions of the notch will be shifted to higher frequencies for an increasing elevation angle, so that the next notch position x_{k+1} can be estimated in relation to the previous one x_k with the help of an underlying state transition model.

4. To further improve the estimation, the detected notches are fitted by the linear approximation $\theta_N = m \cdot \log(f) + n$.

The detected notch frequencies are depicted in Fig. 5 and 6 where the local maxima are marked by a cross and the estimated notches are marked by an open circle. It can be observed that the notch is clearly pronounced for elevation angles $\theta < 0°$ and disappears for larger elevation angles. Although the notch can no longer be detected, the estimated notch is still consistent with less prominent notches up to $\theta = 30°$. In this section, the notches are detected for four azimuth directions $\varphi = [-10°, -30°, -60°, -70°]$ at an elevation angle of $\theta = 0°$, which are later used for the listening experiment. The detection of the tested rear locations $\varphi = [-135°, -165°]$ is difficult since the incident wave from the back does not reflect on a rim of the anti-helix or helix directly, whereby the notch is less pronounced for these directions.
Nevertheless, the subject-averaged notch frequency at $(\theta, \varphi) = (-60°, 60°)$ is located at $f_N = 5.8 \pm 0.5$ kHz and increases to $f_N = 8.0 \pm 0.8$ kHz at $\theta = 0°$. Hence, the first notch is usually larger than 7 kHz and therefore relevant for the confusion rate. In table 3 the difference between the ipsilateral right and left ear notches are depicted. The subject-averaged difference amounts to zero, which indicates no general difference between the ears. The standard deviation of the notch frequencies for all four directions is approximately 0.6 kHz and twice as high as the one of the first resonance. Spagnol and colleagues [18] assume a relationship between the notch frequency f_N and the anthropometric dimension L, which can be expressed as

$$f_N = \frac{c_0}{4L} \tag{3}$$

with the speed of sound c_0. The calculated anthropometric dimension L varies frequency-dependently between 10 and 15 mm for the first notch. In comparison, it is slightly smaller than the dimensions of the cavum concha in table 1 but fits well with the distance to the ear canal entrance. The observed differences between the right and left ear $\Delta f_N = 0.7$ kHz in table 3 refer to deviations of about 1 mm which are very challenging to measure from images or three-dimensional ear models.

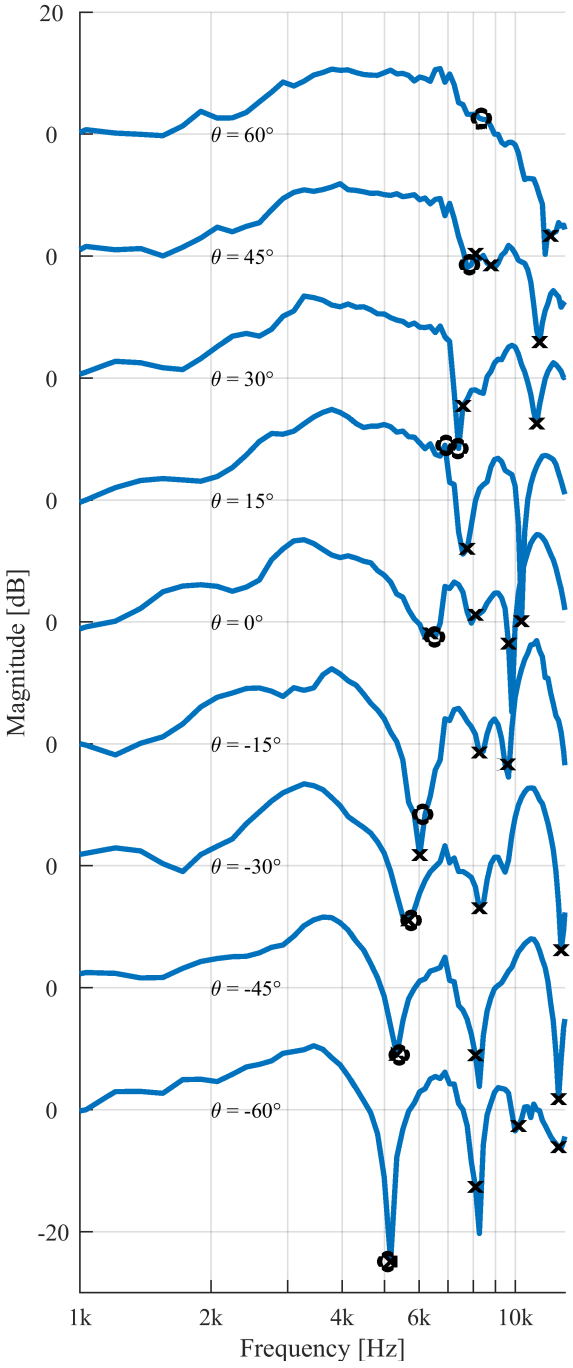


Fig. 5: Ipsilateral HRTFs of data set #33 are plotted for an azimuth angle $\varphi = 10°$ for different elevation angles. The crosses mark detected local minima and the open circles the estimated first notch frequency.

4 Influence on the front-back confusion

One opportunity is to evaluate the front-back confusion rate by means of a localization experiment. Unfortunately, the localization performance is affected by

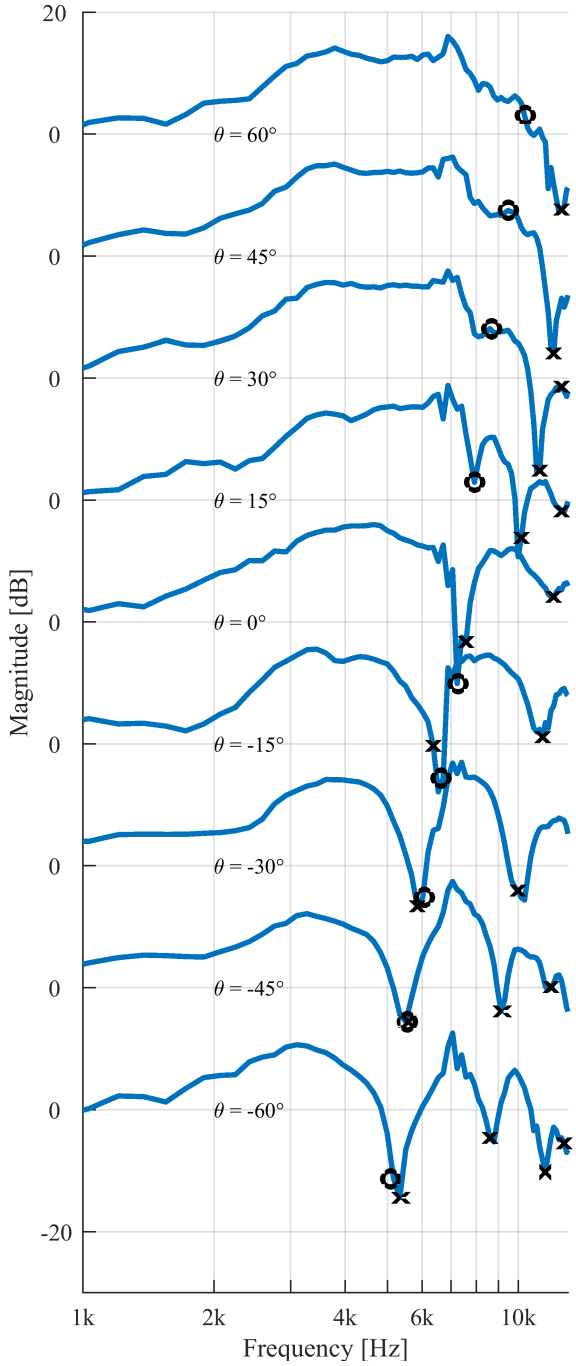


Fig. 6: Ipsilateral HRTFs of data set #33 are plotted for an azimuth angle $\varphi = 60°$ for different elevation angles. The crosses mark detected local minima and the open circles the estimated first notch frequency.

pointing accuracy [19] and at worst, the pointing inaccuracy may mask the investigated factors. Hence, the localization task is reduced to a front-back discrimination to investigate the front-back confusion rate for individual symmetric and asymmetric HRTFs.

The review of the current literature shows that the front-back confusion rate depends on head movements [8, 20, 1, 10, 21, 22], the direction of the incident sound [2, 23], the play-back technique [23, 22] and the listener's experience with the task [23]. The least confusions of frontal and rear locations occur under free-field conditions allowing head movements. Due to the fact that the tested spatial source directions vary in terms of number, direction and listener experience, the rates of Wenzel's comprehensive study [23] are discussed in the following. In contrast to most other above-mentioned studies, this study tested 16 inexperienced listeners under free-field and headphone conditions at 24 spatially-distributed source positions. The subject-averaged confusion rate amounts to 17 $\pm$ 15% in the frontal and 2 $\pm$ 2% in the rear hemisphere under free-field conditions. Reproducing virtual sources via headphones resulted in higher rates of 25 $\pm$ 15% in the frontal and 6 $\pm$ 3% in the rear hemisphere. The inexperienced listeners confused front-back more often than experienced ones in the study. While Wenzel and colleagues used non-individual HRTFs for the reproduction, Bronkhorst [1] reported a lower confusion rate using individual HRTFs. Additionally, he showed that stimuli which do not provide spectral cues above 7 kHz lead to higher confusion rates.

Experimental Setup Seventeen subjects, on average 25 $\pm$ 5 years old, participated in the listening experiment. The individual HRTFs of these subjects were taken from the ITA HRTF database [7]. Three of these subjects were experienced with binaural reproduction techniques. None of the subjects reported hearing loss or damage.

The experiment consisted of four parts (see Fig. 7): reading the instructions, measuring the headphone transfer functions (HpTF) of the subjects, performing the training round and the main experiment.

The HpTFs were measured eight times and averaged according to the procedure of Masiero and Fels [24]. For the measurement Sennheiser HD 650 headphones and KE3 microphones were used. The measured HpTFs were multiplied with the HRTFs (frequency domain) and convolved with a triple-pulsed noise stimulus (time domain). Each pink noise pulse of 150 ms was followed

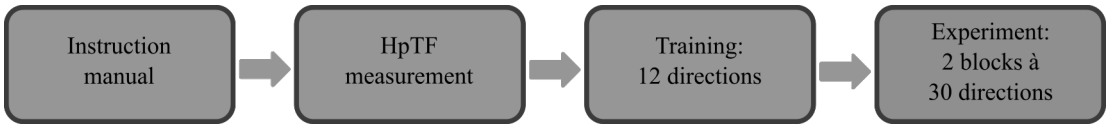


Fig. 7: The four parts of the listening experiment are shown in their chronological order.

by a break of 150 ms. Due to the right ear advantage only directions on the right ear side in the horizontal plane were chosen for the experiment [25]: two in the front ($-10°$ and $-30°$), two at the side ($-60°$ and $-70°$) and two in the rear ($-135°$ and $-165°$).
In the training round three directions of a non-individual HRTF data set were chosen to prepare the subjects for the main task. Apart from this, the procedure of the training round coincided with the one of the main experiment. This consisted of two permuted blocks with asymmetric and symmetric individual HRTFs. The six directions were tested five times in a random order in each block. After the play-back the subject had to choose one of the following options:

1. If the subject perceived the sound from the frontal quadrant, the subject had to choose the button *Front*.
2. If the subject perceived the sound in the rear quadrant, the subject had to choose the button *Rear*.
3. In case that the subject had an in-head or an ambiguously perceived direction, the subject had to choose *Confusion*.

On average, the subjects needed six minutes per block and were able to relax in a short break between both blocks.

Evaluation To evaluate the confusion rate, the numbers of front-back and back-front confusions are added and divided by the total number of trials per direction. Due to an algorithmic mistake in the block with the symmetric HRTFs, only eight subjects remained for the evaluation.
The average confusion rate of the subjects with asymmetric HRTFs is 14% in the front, increases to 59% for lateral directions and drops again to 3% in the rear (see Fig. 8). Such an increased rate for lateral directions can also be found in the study of Makous and Middlebrooks [20]. An explanation for the large lateral rates might be that some subjects defined their interaural axis, which splits the frontal and rear quadrant, in front

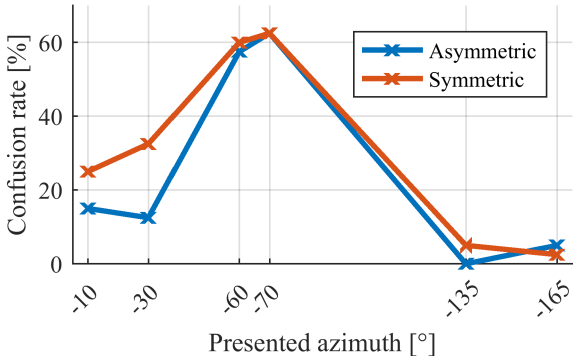


Fig. 8: The front-back confusion rate is plotted against the azimuth angle for asymmetric and symmetric HRTFs (eight subjects). The crosses mark the presented directions.

of their ears. Consequently, these virtual sources close to the interaural axis are rated as sources in the rear. Considering the rates of all 17 subjects for asymmetric HRTFs shows similar rates of 22% in the front, 48% at the sides and 6% in the rear.
Comparing the confusion rates with the asymmetric and symmetric HRTFs (eight subjects), they are very similar for lateral and rear directions (cf. Fig. 8). The missing asymmetry has the highest influence on the frontal confusion rate which rises from 14% to 29%. Repeating each direction five times per subject results in discrete steps of 20%, which is very imprecise for a statistical subject-dependent evaluation. For that reason, a statistical analysis does not show any significance between the HRTF types. However, large standard deviations have also been observed by Wenzel and colleagues [23].
A slight tendency $\rho \approx 0.3$ for all directions in the frontal hemisphere can be observed in such a way that subjects with a larger IESD benefit from their asymmetric HRTFs[1].
Sometimes, the subjects were unable to specify the

[1]The correlation coefficient is calculated from the confusion rates of all 17 subjects using asymmetric HRTFs.

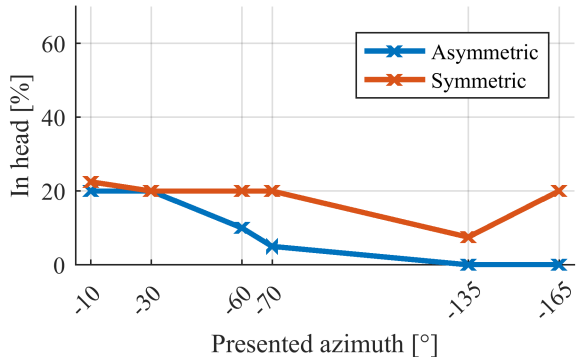


Fig. 9: The in-head localization rate is plotted against the azimuth angle for asymmetric and symmetric HRTFs (eight subjects). The crosses mark the presented directions.

hemisphere or had in-head localizations. This uncertainty on the part of the subjects decreases towards rear directions for both symmetric and asymmetric HRTFs (cf. Fig. 9).
To summarize, the number of front-back confusions is larger for symmetric HRTFs than for asymmetric HRTFs in the front. For lateral and rear positions on the horizontal plane, both are comparable.

5 Summary and conclusion

This paper examined the issue whether the asymmetry of the ear influences the confusion rate. This is an important question, since the measurement effort of anthropometric individualization methods for HRTFs can be reduced, if the confusion rate is not affected by symmetry of the ears.
It can be summarized from literature that the front-back confusion rate increases, if no head movements are allowed and the stimulus to be localized provides no frequencies above 7 kHz [8, 9, 10, 1]. Anthropometric dimensions of the cavum concha, which provide destructive interference effects above 7 kHz, support the auditory system to localize sound sources on the cones of confusion without head movements.
The first resonance frequency of the cavum concha is direction-independent and lower than 7 kHz. For this reason it can be excluded from influencing the confusion rate. The direction-dependent first notch rather influences the confusion rate, since it is forced by dimensions of 10 to 15 mm and located at frequencies around 7 kHz. Deviations of the notch frequency of the right and left ear imply that dimension differences of 1 mm are reasonable.
To investigate the influence of these difference on the confusion rate, six different directions are examined in a listening experiment. The results of this experiment show lower confusion rates for asymmetric HRTFs at frontal directions; the rates at lateral and rear directions are similar for symmetric and asymmetric HRTFs. This suggests that the asymmetry is mandatory for the estimation of HRTFs for reducing the front-back confusions. However, the determination of the corresponding anthropometric dimensions with an accuracy of about 1 mm is very challenging.

References

[1] Bronkhorst, A. W., "Contribution of spectral cues to human sound localization," *The Journal of the Acoustical Society of America*, 98(5), pp. 2542–2553, 1995.

[2] Kistler, D. J. and Wightman, F. L., "A model of head–related transfer functions based on principal components analysis and minimum–phase reconstruction," *The Journal of the Acoustical Society of America*, 91, p. 1637, 1992.

[3] Middlebrooks, J. C., "Individual differences in external-ear transfer functions reduced by scaling in frequency," *The Journal of the Acoustical Society of America*, 106, p. 1480, 1999.

[4] Jin, C., Leong, P., Leung, J., Corderoy, A., and Carlile, S., "Enabling individualized virtual auditory space using morphological measurements," *Proc. First IEEE Pacific-Rim Conf. on Multimedia*, pp. 235–238, 2000.

[5] Inoue, N., Kimura, T., Nishino, T., Itou, K., and Takeda, K., "Evaluation of HRTFs estimated using physical features," *Acoustical science and technology*, 26(5), pp. 453–455, 2005.

[6] Ramos, O. and Tommansini, F., "Magnitude Modelling of HRTF Using Principal Component Analysis Applied to Complex Values," *Archives of Acoustics*, 39(4), pp. 477–482, 2014.

[7] Fels, J. and Bomhardt, R., "A high-resolution head-related transfer function dataset and 3D ear model database," *The Journal of the Acoustical Society of America*, 140(4), p. 3276, 2016.

[8] Wallach, H., "The role of head movements and vestibular and visual cues in sound localization," *Journal of Experimental Psychology*, 27(4), p. 339, 1940.

[9] Roffler, S. K. and Butler, R. A., "Factors that influence the localization of sound in the vertical plane," *The Journal of the Acoustical Society of America*, 43(6), pp. 1255–1259, 1968.

[10] Perrett, S. and Noble, W., "The effect of head rotations on vertical plane sound localization," *The Journal of the Acoustical Society of America*, 102(4), pp. 2325–2332, 1997.

[11] Shaw, E. A. G. and Teranishi, R., "Sound Pressure Generated in an External–Ear Replica and Real Human Ears by a Nearby Point Source," *The Journal of the Acoustical Society of America*, 44(1), pp. 240–249, 1968.

[12] Spagnol, S. and Geromazzo, M., "Estimation and modeling of pinna-related transfer functions," *13th Int. Conference on Digital Audio Effects, Graz, Austria*, 2010.

[13] Satarzadeh, P., Algazi, V. R., and Duda, R. O., "Physical and filter pinna models based on anthropometry," *Audio Engineering Convention 122, Vienna, Austria*, 2007.

[14] Algazi, V. R., Duda, R. O., and Thompson, D. M., "The CIPIC HRTF database," *Applications of Signal Processing to Audio and Acoustics, IEEE Workshop*, 2001, 2001.

[15] Genovese, A. F., Juras, J., Miller, C., and Roginska, A., "The Effect of Elevation on ITD Symmetry," *Audio Engineering Conference, Aalborg, Denmark*, 2016.

[16] Mokhtari, P., Takemoto, H., Nishimura, R., and Kato, H., "Frequency and amplitude estimation of the first peak of head-related transfer functions from individual pinna anthropometry," *The Journal of the Acoustical Society of America*, 137(2), pp. 690–701, 2015.

[17] Raykar, V. C., Duraiswami, R., and Yegnanarayana, B., "Extracting the frequencies of the pinna spectral notches in measured head related impulse responses," *The Journal of the Acoustical Society of America*, 118(1), pp. 364–374, 2005.

[18] Spagnol, S., Geronazzo, M., and Avanzini, F., "On the relation between pinna reflection patterns and head-related transfer function features," *IEEE Transactions on audio, speech, and language processing, Vol. 21*, 21(3), pp. 508–519, 2013.

[19] Bahu, H., Carpentier, T., Noisternig, M., and Warusfel, O., "Comparison of Different Egocentric Pointing Methods for 3D Sound Localization Experiments," *Acta Acustica united with Acustica*, 102(1), pp. 107–118, 2016.

[20] Makous, J. C. and Middlebrooks, J. C., "Two–dimensional sound localization by human listeners," *The Journal of the Acoustical Society of America*, 87(5), pp. 2188–2200, 1990.

[21] Wightman, F. L. and Kistler, D. J., "Resolution of front–back ambiguity in spatial hearing by listener and source movement," *The Journal of the Acoustical Society of America*, 105(5), pp. 2841–2853, 1999.

[22] Hill, P. A., Nelson, P. A., Kirkeby, O., and Hamada, H., "Resolution of front–back confusion in virtual acoustic imaging systems," *The Journal of the Acoustical Society of America*, 108(6), pp. 2901–2910, 2000.

[23] Wenzel, E. M., Arruda, M., Kistler, D. J., and Wightman, F. L., "Localization using nonindividualized head–related transfer functions," *The Journal of the Acoustical Society of America*, 94, p. 111, 1993.

[24] Masiero, B. and Fels, J., "Perceptually robust headphone equalization for binaural reproduction," *Audio Engineering Society Convention 130, London, UK*, 2011.

[25] Emmerich, D. S., Harris, J., Brown, W. S., and Springer, S. P., "The relationship between auditory sensitivity and ear asymmetry on a dichotic listening task," *Neuropsychologia*, 26(1), pp. 133–143, 1988.